International Research Journal of Innovations in Engineering and Technology (IRJIET)

ISSN (online): 2581-3048

Volume 9, Issue 6, pp 171-175, June-2025

https://doi.org/10.47001/IRJIET/2025.906023

Micro-Rotation Error Due to Base Angle Vibration

Mai Anh Phạm

Faculty of Basic Sciences, Hanoi University of Mining and Geology, No. 18 Viên street, BacTuLiem district, Hanoi, Vietnam

***Abstract* - This article studies the mathematical model of the oscillation behavior of a micromechanical gyroscope under angular vibrations of the base. The motion equations are presented in the form of the Mathew-Hill differential equations. By applying the Krylov-Bogolyubov averaging method to analyze the slow-variable dynamics of the gyroscope, it is found that angular base vibrations occurring at resonant frequencies significantly affect the accuracy of the gyroscopic measurement.**

Keywords: dynamics, micro-gyro, vibration, microelectromechanical, accuracy of micro-gyro.

I. Introduction

Over the past 30 years, the emergence and development of microelectromechanical systems (MEMS)—a high-tech field—has sparked a revolution in science and technology by enabling the fabrication of sensors and actuators at the sub-millimeter scale. Among these, the micromechanical gyroscope (also known as a micro gyroscope) has shown great promise and is increasingly being applied in precision navigation and stabilization systems, such as aerospace vehicles, satellite antennas, optoelectronic devices, automotive systems, and household appliances. Consequently, improving the accuracy of micro gyroscopes is a critical issue that has drawn attention from both domestic and international researchers.

The foundation for designing and enhancing the accuracy of micro gyroscopes lies in the development of mathematical models that describe the nonlinear dynamic behavior of the sensitive elements.

A micromechanical gyroscope is essentially an electromechanical system based on vibrational motion. In this article, the author examines an RR-type micro gyroscope (based on Boxenhorn B.'s invention [1,4]), focusing on the angular motion of the inner sensing element. The gyroscope structure is created using a 300-micrometer-thick silicon layer and photolithographic techniques, as illustrated in Figure 1.

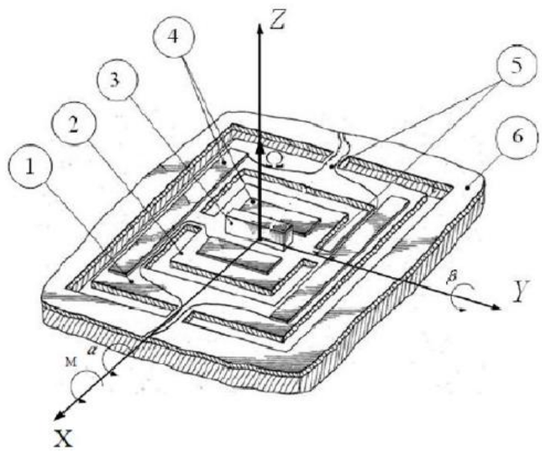

Figure 1: Structure of an RR-type micromechanical gyroscope
1 - Outer frame. 2 - Inner frame. 3 - Sensing element. 4 - Electrodes. 5 - Torsion bar. 6 - Base support.

II. Dynamics of the Sensing Element in an RR-Type Micromechanical Gyroscope under Angular Base Vibrations

2.1 Mathematical Model

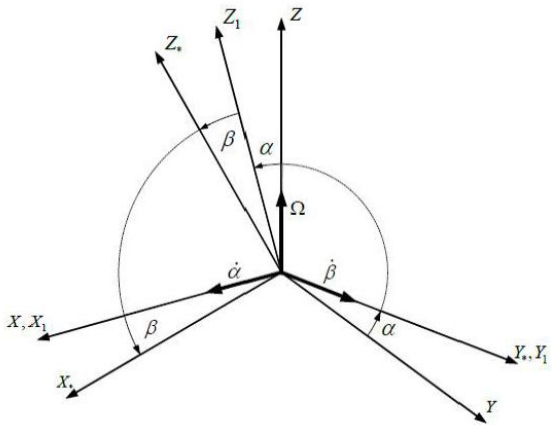

Figure 2: Coordinate system

Figure 2 describes the coordinate systems used:

- The Oxyz system is attached to the base of the gyroscope. Axis Ox coincides with the outer frame's rotation axis, Oy with the inner frame's axis, and Oz completes the right-handed coordinate system.

ISSN (online): 2581-3048
Volume 9, Issue 6, pp 171-175, June-2025
https://doi.org/10.47001/IRJIET/2025.906023

- The $Ox_1y_1z_1$ system is attached to the outer frame. Axis Ox_1 aligns with its rotation axis, Oy_1 with the inner frame's axis, and Oz_1 completes the right-handed system.
- The Oxyz* system is aligned with the primary symmetry axis of the sensing element, where Ox* matches the outer rotation axis, Oy* with the inner frame, and Oz* completes the right-handed system.

Let:

- **Ω** – angular velocity of the base,
- **α** – angular displacement of the outer frame relative to the base,
- **β** – angular displacement of the sensing element (inner frame) relative to the outer frame.

We can describe the transformation between coordinate systems [2]:

$$Oxyz \xrightarrow[x]{\alpha} Ox_1y_1z_1 \xrightarrow[y_1]{\beta} Ox_*y_*z_* . \quad (1)$$

Using kinetic energy equations and angular velocity vectors:

$$T = \frac{1}{2}\mathbf{\Omega}_*^{\mathbf{T}} \cdot \mathbf{J} \cdot \mathbf{\Omega}_* + \frac{1}{2}\mathbf{\Omega}_\alpha^{\mathbf{T}} \cdot \mathbf{I} \cdot \mathbf{\Omega}_\alpha , \quad (2)$$

Where:

- **Ω*** is the angular velocity vector of the sensing element,
- **J** is the moment of inertia matrix of the sensing element with respect to Oxyz,
- **ω_α** is the angular velocity of the outer frame in the Oxyz system,
- **I** is the moment of inertia matrix of the inner and outer frames in $Ox_1y_1z_1$,
- It is assumed the products of inertia are zero.

Thus, the system's kinetic energy is:

$$T = \frac{1}{2}\Big[J_x\left(\dot{\alpha}\cos\beta - \Omega\cos\alpha\sin\beta\right)^2 + J_y\left(\Omega\sin\alpha + \dot{\beta}\right)^2 + \\ + J_z\left(\Omega\cos\alpha\cos\beta + \dot{\alpha}\sin\beta\right)^2 + I_x\dot{\alpha}^2 + I_y\Omega^2\sin^2\alpha + I_z\Omega^2\cos^2\alpha\Big]. \quad (3)$$

Elastic potential energy:

$$\Pi = \frac{1}{2}c_\alpha\alpha^2 + \frac{1}{2}c_\beta\beta^2 - M\alpha , \quad (4)$$

Where:

- $\mathbf{c_\alpha}$, $\mathbf{c_\beta}$ – torsional stiffness coefficients for the outer and inner frames,
- **M** – restoring moment.

Dissipated energy:

$$\Phi = \frac{1}{2}k_\alpha\dot{\alpha}^2 + \frac{1}{2}k_\beta\dot{\beta}^2 \quad (5)$$

Where:

- $\mathbf{k_\alpha}$, $\mathbf{k_\beta}$ – damping coefficients.

Using the second form of Lagrange's equations and neglecting higher-order rigid body terms, we obtain the system of equations

$$\begin{cases} \left(I_x + J_x\right)\ddot{\alpha} + \left(J_z - J_x\right)\ddot{\alpha}\beta^2 + 2\left(J_z - J_x\right)\beta\dot{\alpha}\dot{\beta} - \left(J_x + J_y - J_z\right)\dot{\beta}\Omega + \\ + \left(J_z - J_x\right)\beta\dot{\Omega} + \left(I_z - I_y + J_z - J_y\right)\alpha\Omega^2 + k_\alpha\dot{\alpha} + c_\alpha\alpha + M = 0, \\ J_y\ddot{\beta} + \left(J_x - J_z\right)\beta\dot{\alpha}^2 + \left(J_x + J_y - J_z\right)\dot{\alpha}\Omega + \\ + \left(J_z - J_x\right)\beta\Omega^2 + J_y\dot{\Omega}\alpha + c_\beta\beta + k_\beta\dot{\beta} = 0. \end{cases} \quad (6)$$

Equation 6isin the original paper, which represents the physical model describing the dynamics of the sensing element in the micro gyroscope.

To simplify the analysis without altering the system's properties, non-dimensional variables and slow time are introduced:

$$\tau = \omega t,\ \alpha = \sqrt{\varepsilon}\sqrt{j_1}x,\ \beta = \sqrt{\varepsilon}\sqrt{j_2}y,\ \omega = \sqrt{\frac{c_\beta}{J_y}} = \sqrt{\frac{c_\alpha}{J_x + I_x}},$$

$$\varepsilon\gamma = \frac{k_\alpha}{\sqrt{c_\alpha\left(J_x + I_x\right)}} = \frac{k_\beta}{\sqrt{c_\beta J_y}}, \varepsilon\nu = \sqrt{j_1}\sqrt{j_2}\frac{\Omega}{\omega},\ m\varepsilon^{3/2} = \frac{M}{c_\alpha}\sqrt{\frac{J_x + I_x}{J_x + J_y - J_z}}$$

$$j_1 = \frac{J_x + J_y - J_z}{J_x + I_x} > 0,\ j_2 = \frac{J_x + J_y - J_z}{J_y} > 0,\ \xi = \frac{1}{j_2}, \quad (7)$$

Where:

$\Omega-$ the natural oscillation frequency of the inductive element;
γ_1, γ_2- the corresponding vibration coefficients of the internal and external stands;
J_1 ,J_2, J, ξ $-$parameters characterizing the massand geometry of the micro-rotating gyrosensor,
M $-$forced moment

Substituting expression (7) into equations system (6) we get:

$$\begin{cases} \ddot{x} + x = \varepsilon\left(-\gamma\dot{x} + \nu\dot{y} + \left(1 - \xi\right)\dot{\nu}\,y - m\right), \\ \ddot{y} + y = \varepsilon\left(-\gamma\dot{y} - \nu\dot{x} - \xi\dot{\nu}\,x\right). \end{cases} \quad (8)$$

Equations system (8) is a mathematical model describing the motion of the micro-gyro sensor.

International Research Journal of Innovations in Engineering and Technology (IRJIET)

ISSN (online): 2581-3048

Volume 9, Issue 6, pp 171-175, June-2025

https://doi.org/10.47001/IRJIET/2025.906023

2.2 Angular Vibration of the Base – Problem Statement

We study the dynamic behavior of the sensing element under the condition that the base of the gyroscope undergoes angular oscillation. The angular velocity of the base is assumed to be:

$$\Omega = \Omega_0 + \Omega_1 \sin(2\omega_0 t) \qquad (9)$$

Where:

- Ω_0: constant angular velocity of the base,
- Ω_1: amplitude of the base's angular oscillation,
- $2\omega_0$: frequency of base oscillation.

Transforming into non-dimensional form using definitions from earlier:

$$\nu = \nu_0 + \nu_1 \sin(2\mu\tau) \qquad (10)$$

Where:

$$\varepsilon\nu_0 = \sqrt{J_1}\sqrt{J_2}\frac{\Omega_0}{\omega}, \varepsilon\nu_1 = \sqrt{J_1}\sqrt{J_2}\frac{\Omega_1}{\omega}, \mu = \frac{\omega_0}{\omega} \quad (10)$$

Substituting expression (10) into equation system (8) we get:

$$\begin{cases} \ddot{x} + x = \varepsilon\left(-\gamma\dot{x} + \left(\nu_0 + \nu_1 \sin 2\mu\tau\right)\dot{y} + 2\mu\left(1-\xi\right)\nu_1 y\cos 2\mu\tau - m_0 \sin\mu\tau\right), \\ \ddot{y} + y = \varepsilon\left(-\gamma\dot{y} - \left(\nu_0 + \nu_1 \sin 2\mu\tau\right)\dot{x} - 2\mu\xi\nu_1 x\cos 2\mu\tau\right). \end{cases} \quad (11)$$

Substituting into the non-dimensional system of equations yields a second-order differential system (Equation 11), which takes the form of a **Mathieu-Hill differential equation**.

We analyze the system under **resonance conditions**, where the frequency of angular base vibration is approximately twice the natural frequency of the sensing element:

$$\mu = 1 - \varepsilon\lambda \qquad (12)$$

Where:

- λ: detuning parameter ($\lambda \sim 1$)

To analyze the slow variation of the system's response phase under resonance, we transform the original variables x, x, y, y into **slow-varying variables**p_1, q_1, p_2, q_2 using the Van der Pol transformation:

$$\begin{aligned} x &= q_1\cos\mu\tau + p_1\sin\mu\tau \\ \dot{x} &= -q_1\mu\sin\mu\tau + p_1\mu\cos\mu\tau \\ y &= q_2\cos\mu\tau + p_2\sin\mu\tau \\ \dot{y} &= -q_2\mu\sin\mu\tau + p_2\mu\cos\mu\tau \end{aligned} \qquad (13)$$

Based on the main parameters (12), the system of equations (11) after being transformed into the slow variables 1 1 2 2 p , q , p , q according to the formulas (13), we get the system of gyrodynamic equations according to the slow variable. Applying the Krylov-Bogoliubov averaging method to study the system of dynamic equations of a gyroscope with a slow-moving vibration occurring at the resonance frequency [3], we obtain the following system of equations:

$$\begin{cases} \dot{q}_1 = \varepsilon\left(-2\gamma q_1 - 4\lambda p_1 + 2\nu_0 q_2 - \left(2\xi - 1\right)\nu_1 p_2 - 2m_0\right)/4, \\ \dot{p}_1 = \varepsilon\left(-2\gamma p_1 + 4\lambda q_1 + 2\nu_0 p_2 - \left(2\xi - 1\right)\nu_1 q_2\right)/4, \\ \dot{q}_2 = \varepsilon\left(-2\gamma q_2 - 4\lambda p_2 - 2\nu_0 q_1 - \left(2\xi - 1\right)\nu_1 p_1\right)/4, \\ \dot{p}_2 = \varepsilon\left(-2\gamma p_2 + 4\lambda q_2 - 2\nu_0 p_1 - \left(2\xi - 1\right)\nu_1 q_1\right)/4. \end{cases}, \quad (14)$$

To facilitate the solution of the system of differential equations (14), we introduce the new base displacement quantity:

$$\nu_{1*} = \frac{1}{2}(2\xi - 1)\nu_1, \left(2\xi - 1 = \frac{J_y + J_z - J_x}{J_x + J_y - J_z} > 0\right), \quad (15)$$

We get the new system of equations with the slow variable:

$$\begin{cases} \dot{q}_1 = \varepsilon\left(-\gamma q_1 - 2\lambda p_1 + \nu_0 q_2 - \nu_{1*} p_2 - m_0\right)/2, \\ \dot{p}_1 = \varepsilon\left(-\gamma p_1 + 2\lambda q_1 + \nu_0 p_2 - \nu_{1*} q_2\right)/2, \\ \dot{q}_2 = \varepsilon\left(-\gamma q_2 - 2\lambda p_2 - \nu_0 q_1 - \nu_{1*} p_1\right)/2, \\ \dot{p}_2 = \varepsilon\left(-\gamma p_2 + 2\lambda q_2 - \nu_0 p_1 - \nu_{1*} q_1\right)/2. \end{cases}, \quad (16)$$

In the next section, we will ignore the asterisk (*) to present a simple formula. Solving the system of differential equations (16), we get the following solutions:

$$\begin{cases} q_1(\tau) = \left(\left(p_{20} + q_{10}\right)\lambda_4 + \left(p_{10} - q_{20}\right)\lambda_5\right)e_1 + \left(\left(q_{10} - p_{20}\right)\lambda_3 + \left(p_{10} + q_{20}\right)\lambda_6\right)e_2 + \\ \quad + \left(\left(q_{10} - p_{20}\right)\lambda_2 - \left(p_{10} + q_{20}\right)\lambda_6\right)e_3 + \left(\left(p_{20} + q_{10}\right)\lambda_1 + \left(q_{20} - p_{10}\right)\lambda_5\right)e_4 + \\ \quad + \left(\frac{\lambda_4 e_1}{\lambda_7} + \frac{\lambda_3 e_2}{\lambda_8} + \frac{\lambda_2 e_3}{\lambda_9} + \frac{\lambda_1 e_4}{\lambda_{10}} - \frac{\lambda_{11}}{\lambda_7\lambda_8\lambda_9\lambda_{10}}\right)m_0, \\ p_1(\tau) = \left(\left(p_{10} - q_{20}\right)\lambda_1 - \left(p_{20} + q_{10}\right)\lambda_5\right)e_1 + \left(\left(p_{10} + q_{20}\right)\lambda_2 + \left(p_{20} - q_{10}\right)\lambda_6\right)e_2 \\ \quad + \left(\left(p_{10} + q_{20}\right)\lambda_3 + \left(q_{10} - p_{20}\right)\lambda_6\right)e_3 + \left(\left(p_{10} - q_{20}\right)\lambda_4 + \left(p_{20} + q_{10}\right)\lambda_5\right)e_4 \\ \quad + \left(-\frac{\lambda_5 e_1}{\lambda_7} - \frac{\lambda_6 e_2}{\lambda_8} + \frac{\lambda_6 e_3}{\lambda_9} + \frac{\lambda_5 e_4}{\lambda_{10}} - \frac{\lambda_{12}}{\lambda_7\lambda_8\lambda_9\lambda_{10}}\right)m_0, \\ q_2(\tau) = \left(\left(q_{20} - p_{10}\right)\lambda_1 + \left(p_{20} + q_{10}\right)\lambda_5\right)e_1 + \left(\left(p_{10} + q_{20}\right)\lambda_2 + \left(p_{20} - q_{10}\right)\lambda_6\right)e_2 + \\ \quad + \left(\left(p_{10} + q_{20}\right)\lambda_3 + \left(q_{10} - p_{20}\right)\lambda_6\right)e_3 + \left(\left(q_{20} - p_{10}\right)\lambda_4 - \left(p_{20} + q_{10}\right)\lambda_5\right)e_4 + \\ \quad + \left(\frac{\lambda_5 e_1}{\lambda_7} - \frac{\lambda_6 e_2}{\lambda_8} + \frac{\lambda_6 e_3}{\lambda_9} - \frac{\lambda_5 e_4}{\lambda_{10}} + \frac{\lambda_{12}}{\lambda_7\lambda_8\lambda_9\lambda_{10}}\right)m_0, \\ p_2(\tau) = \left(\left(p_{20} + q_{10}\right)\lambda_4 + \left(p_{10} - q_{20}\right)\lambda_5\right)e_1 + \left(\left(p_{20} - q_{10}\right)\lambda_3 - \left(p_{10} + q_{20}\right)\lambda_6\right)e_2 \\ \quad + \left(\left(p_{20} - q_{10}\right)\lambda_2 + \left(p_{10} + q_{20}\right)\lambda_6\right)e_3 + \left(\left(p_{20} + q_{10}\right)\lambda_1 + \left(q_{20} - p_{10}\right)\lambda_5\right)e_4 \\ \quad + \left(\frac{\lambda_4 e_1}{\lambda_7} - \frac{\lambda_3 e_2}{\lambda_8} - \frac{\lambda_2 e_3}{\lambda_9} + \frac{\lambda_1 e_4}{\lambda_{10}} + \frac{\lambda_{14}}{\lambda_7\lambda_8\lambda_9\lambda_{10}}\right)m_0. \end{cases} \quad (17)$$

International Research Journal of Innovations in Engineering and Technology (IRJIET)

ISSN (online): 2581-3048

Volume 9, Issue 6, pp 171-175, June-2025

https://doi.org/10.47001/IRJIET/2025.906023

In which

$$e_{1,4} = \frac{e^{-\varepsilon\left(\gamma \pm \sqrt{\nu_1^2-(2\lambda+\nu_0)^2}\right)\tau/2}}{4\sqrt{\nu_1^2-(2\lambda+\nu_0)^2}},\ e_{2,3} = \frac{e^{-\varepsilon\left(\gamma \pm \sqrt{\nu_1^2-(2\lambda-\nu_0)^2}\right)\tau/2}}{4\sqrt{\nu_1^2-(2\lambda-\nu_0)^2}},$$
$$\lambda_{1,4}=\sqrt{\nu_1^2-(2\lambda+\nu_0)^2} \mp \nu_1,\ \lambda_{2,3}=\sqrt{\nu_1^2-(2\lambda-\nu_0)^2} \pm \nu_1, \lambda_{5,6}=2\lambda \pm \nu_0,$$
$$\lambda_{7,10}=\gamma \pm \sqrt{\nu_1^2-(2\lambda+\nu_0)^2}, \lambda_{8,9}=\gamma \pm \sqrt{\nu_1^2-(2\lambda-\nu_0)^2}, \quad ,$$
$$\lambda_{11}=4\nu_1\lambda\nu_0+\gamma\left(\gamma^2-\nu_1^2+4\lambda^2+\nu_0^2\right), \lambda_{12}=2\lambda\left(\gamma^2-\nu_1^2+4\lambda^2-\nu_0^2\right),$$
$$\lambda_{13}=2\nu_0\left(\gamma^2-\nu_1^2-4\lambda^2+\nu_0^2\right), \lambda_{14}=4\gamma\nu_0\lambda+\nu_1\left(\gamma^2-\nu_1^2+4\lambda^2+\nu_0^2\right). \quad (18)$$

III. Gyroscope Error under Angular Base Vibration Conditions

We obtain information about the angular displacements **α** and **β** of the micromechanical gyroscope's sensing element through static electrical electrodes, which effectively correspond to the variables p_1, q_1, p_2, q_2. This reflects the physical basis of the Krylov–Bogolyubov averaging method applied in this study.

To determine the base's angular velocity, the following equation from reference [2] is used:

$$\tan(2\theta) = \frac{q_1 q_2 + p_1 p_2}{q_1^2 + p_1^2 - q_2^2 - p_2^2} \qquad (19)$$

Where:

- **θ** is the precession angle, which is proportional to the integral of the base's angular velocity.

To assess the gyroscope error caused by angular base oscillation under resonance, we compute the time derivative of the function $\theta = \frac{1}{2}$arctan based on Equation (18). Substituting the time derivatives $\dot{p}_1, \dot{q}_1, \dot{p}_2, \dot{q}_2$ from the dynamic system (Equation 15), we get:

$$\dot{\theta} = \frac{1}{2}\frac{d}{d\tau} arctg\left(\frac{2(q_1q_2+p_1p_2)}{q_1^2+p_1^2-q_2^2-p_2^2}\right) =$$
$$= -\frac{1}{2}\varepsilon\left(\nu_0+\nu_1\frac{(p_1q_1+p_2q_2)\left(p_1^2-p_2^2+q_1^2-q_2^2\right)}{\left((p_2+q_1)^2+(p_1-q_2)^2\right)\left((p_2-q_1)^2+(p_1+q_2)^2\right)}-\right.,$$
$$\left.-\frac{m_0\left(q_2\left(q_1^2-p_1^2+q_2^2+p_2^2\right)+2p_1p_2q_1\right)}{\left((p_2+q_1)^2+(p_1-q_2)^2\right)\left((p_2-q_1)^2+(p_1+q_2)^2\right)}\right). \qquad (20)$$

This expression shows that in the case of **resonance** (when the base's angular vibration frequency approaches twice the natural frequency of the sensing element), the precession angular velocity $\dot{\theta}$— and thus the error—increases. This error depends on:

- The base's mean angular velocity ν_0,
- The amplitude of angular base vibration ν_1,
- The solution of the slow-varying system (Equation 16).

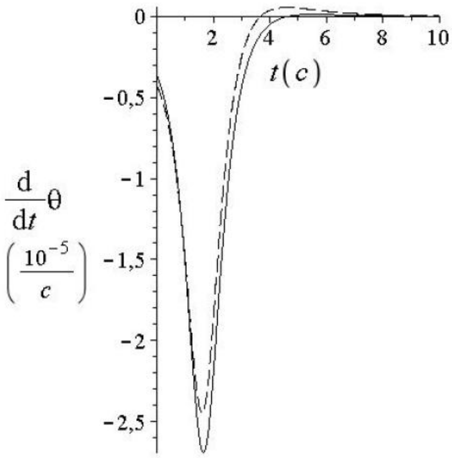

Figure 3: the angular velocity of the moving object according to formula (17) (solid line) and the angular velocity of the moving object (solid line)

Using sample parameters for the RR-type micromechanical gyroscope from reference [5]:

- Torsional stiffness:

$$c_\alpha = c_\beta = 8.48 \times 10^{-5}\ \mathrm{Nm}$$

- Moment of inertia:

$$J_x = J_y = J_z = I_x = 2.4 \times 10^{-13}\ \mathrm{kg \cdot m^2}$$

- Dimensionless geometric and mass parameters:

$$j_1 = 1, j_2 = 3/2, j_3 = 1/2, \xi = 2/3$$

- Natural oscillation frequency of the sensing element:

$$\omega = 1.88 \times 10^4\ \mathrm{rad/s}$$

- Amplitude of angular base vibration:

$$\Omega_1 = 2 \times 10^{-6}\ \mathrm{rad/s}$$

With these values, the maximum precession angular velocity error calculated from Equation (19) is:

$$\Delta\dot{\theta} = 2.8 \times 10^{-6}\ \mathrm{rad/s}$$

IV. Conclusions

The study of the dynamics of micromechanical gyroscopes is essential for the design, fabrication, and development of applications aiming to improve their accuracy in operation. In this paper, the dynamics of an RR-type micromechanical gyroscope under the influence of angular vibration from the base have been analyzed.

ISSN (online): 2581-3048
Volume 9, Issue 6, pp 171-175, June-2025
https://doi.org/10.47001/IRJIET/2025.906023

The analysis concludes that under **resonance conditions**—when the angular vibration frequency of the base approaches **half of the sensing element's natural frequency**—**excitation phenomena** occur. Specifically, base angular vibration under resonance leads to an **increase in the error** of the micromechanical gyroscope.

The formula derived in this study (Equation 17) can be used to accurately **quantify the gyroscope error** when mounted on a base undergoing angular vibration under various conditions. These results are applicable in the **design**, **manufacture**, and **experimental testing** of micromechanical gyroscopes.

REFERENCES

[1] Boxenhorn B., "Planar inertial sensor" United States Patent No. 4,598,585. July 8, 1986M. Young, The Technical Writer's Handbook. *Mill Valley, CA: University Science, 1989. International Class:* G01P 015/02.

[2] Schwerin, R.: Multibody System Simulation. Numerical Methods, Algorithms and Software. *Springer*, Berlin (1999)

[3] Udwadia, F.E., Phohomsiri, P.: Explicit equations of motion for constrained mechanical systems with singular mass matrices and applications to multi-body dynamics. *Proc. R. Soc. A, Math. Phys. Eng. Sci.* 462(2071), 2097–2117 (2006).

Citation of this Article:

Mai Anh Phạm. (2025). Micro-Rotation Error Due to Base Angle Vibration. *International Research Journal of Innovations in Engineering and Technology - IRJIET*, 9(6), 171-175. Article DOI https://doi.org/10.47001/IRJIET/2025.906023

****